

END-TO-END DEEP LEARNING-BASED ADAPTATION CONTROL FOR FREQUENCY-DOMAIN ADAPTIVE SYSTEM IDENTIFICATION

Thomas Haubner, Andreas Brendel, and Walter Kellermann

Multimedia Communications and Signal Processing, Friedrich-Alexander-University Erlangen-Nürnberg,
Cauerstr. 7, D-91058 Erlangen, Germany, thomas.haubner@fau.de

ABSTRACT

We present a novel end-to-end deep learning-based adaptation control algorithm for frequency-domain adaptive system identification. The proposed method exploits a deep neural network to map observed signal features to corresponding step-sizes which control the filter adaptation. The parameters of the network are optimized in an end-to-end fashion by minimizing the average normalized system distance of the adaptive filter. This avoids the need of explicit signal power spectral density estimation as required for model-based adaptation control and further auxiliary mechanisms to deal with model inaccuracies. The proposed algorithm achieves fast convergence and robust steady-state performance for scenarios characterized by high-level, non-white and non-stationary additive noise signals, abrupt environment changes and additional model inaccuracies.

Index Terms— System Identification, Adaptation Control, Deep Learning, Frequency-Domain Adaptive Filtering

1. INTRODUCTION

Adaptive system identification is required for many modern signal enhancement approaches, e.g., in full-duplex acoustic communication devices for the purpose of acoustic echo cancellation (AEC) [1]. Despite the recently increased focus on direct deep learning-based signal enhancement algorithms [2, 3], the benefit of additionally using model-based system identification has shown to be beneficial, especially when computational load should be minimized [4, 5].

However, the benefits of physical models are only fully exploited if their optimum model parameters can be quickly and robustly identified. For this, gradient descent-based model parameter updates have proven to be a powerful approach [6, 7] when combined with carefully-designed adaptation control to deal with interfering signals and noise (jointly termed ‘noise’ in the sequel) [8] and model inaccuracies, e.g., undermodeling the filter length [9]. During the last decades a plethora of adaptation control methods have been proposed, ranging from simplistic binary stall-or-adapt approaches [10, 11] to sophisticated model-based step-size estimators [12, 13, 14, 15] and learning-based combination of step-size selection schemes [16]. Most adaptation control approaches assume simplifying probabilistic signal models to estimate a time-varying step-size by minimizing the mean squared error signal or a system distance between the estimated frequency response (FR) and the true FR. In particular the frequency-selective step-size inference by a diagonalized discrete Fourier transform (DFT)-domain Kalman filter (KF) [17] performs robustly in scenarios challenged by non-white and non-stationary additive noise signals. However,

the performance of these model-based approaches depends on the validity of the model assumptions and robust estimation of the required statistics [18]. Especially the estimation of statistics corresponding to unobserved quantities, e.g., the noise power spectral density (PSD), poses a difficult problem [18]. Various estimators have been proposed, e.g., [19, 20, 21], whose performance often crucially depends on the choice of additional hyperparameters and the considered application. Recently, the exploitation of machine learning-based noise PSD estimators [5, 22] has shown significant improvements relative to classical, i.e., non-trainable, estimators. Yet, these approaches still rely on simplistic random walk models to describe the temporal evolution of the FR [17] and require a sophisticated cost function design for PSD estimation [23].

Thus, we introduce in this paper an end-to-end deep learning-based adaptation control algorithm for frequency-domain adaptive system identification which we term deep neural network-controlled frequency-domain adaptive filter (DNN-FDAF). We propose to learn a mapping from observable signal features to step-sizes by a DNN with the average normalized Euclidean system distance (NESD) of the step-size-controlled adaptive filter as a loss function. By optimizing the DNN parameters directly w.r.t. the NESD, we avoid the estimation of auxiliary signal statistics for model-based adaptation control whose effect on the system identification performance depends on the validity of the assumed model properties. In addition, it circumvents the need for application-dependent hyperparameter tuning inherent to many baseline approaches. The proposed method combines the benefits of physically-motivated system identification approaches, e.g., generalization to unknown environments, with the excellent modeling capability of DNNs for adaptation control.

We use bold lowercase letters for vectors and bold uppercase letters for matrices with underlined symbols indicating time-domain quantities. The identity matrix and DFT matrix of dimensions $D \times D$ are denoted by \mathbf{I}_D and \mathbf{F}_D , respectively, and the all-zero matrix of dimensions $D_1 \times D_2$ by $\mathbf{0}_{D_1 \times D_2}$. Furthermore, we introduce the $\text{diag}(\cdot)$ operator which generates a diagonal matrix from its vector-valued argument and indicate its m th element by $[\cdot]_{mm}$. The transposition and Hermitian transposition of a matrix are represented by $(\cdot)^T$ and $(\cdot)^H$, respectively. Finally, we use the Euclidean norm $\|\cdot\|_2$ and the expectation operator $\mathbb{E}[\cdot]$.

2. ADAPTIVE SYSTEM IDENTIFICATION

In the following, the online identification of an acoustic model describing the multi-path propagation from a source, e.g., a loudspeaker, to a microphone as shown in Fig. 1 is considered. We model a block of noisy microphone observations at block index τ

$$\underline{\mathbf{y}}_\tau = \left(\underline{y}_{\tau R-R+1}, \underline{y}_{\tau R-R+2}, \dots, \underline{y}_{\tau R} \right)^T \in \mathbb{R}^R \quad (1)$$

This work was supported by the German Research Foundation - 282835863 - within the Research Unit FOR2457 Acoustic Sensor Networks.

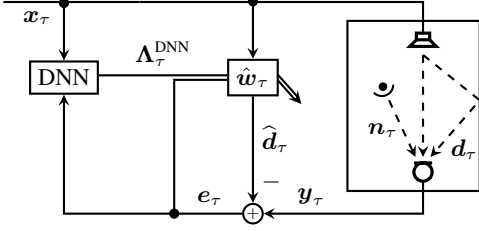


Fig. 1: Block diagram of the proposed DNN-FDAF algorithm for online system identification.

as a linear superposition

$$\underline{y}_\tau = \underline{d}_\tau + \underline{n}_\tau \in \mathbb{R}^R \quad (2)$$

of a noise-free observation component \underline{d}_τ and a noise component \underline{n}_τ . The noise-free observation component \underline{d}_τ is described by a linear convolution of an observable input signal block

$$\underline{x}_\tau = (\underline{x}_{\tau R-M+1}, \underline{x}_{\tau R-M+2}, \dots, \underline{x}_{\tau R})^T \in \mathbb{R}^M \quad (3)$$

with a finite impulse response (FIR) filter $\underline{w}_\tau \in \mathbb{R}^L$ of length $L = M - R$ modeling the multi-path propagation. The linear convolution can efficiently be implemented by overlap-save processing in the DFT domain

$$\underline{d}_\tau = \mathbf{Q}_1^T \mathbf{F}_M^{-1} \mathbf{X}_\tau \mathbf{w}_\tau \in \mathbb{R}^R, \quad (4)$$

with the FR $\mathbf{w}_\tau = \mathbf{F}_M \mathbf{Q}_2 \underline{w}_\tau \in \mathbb{C}^M$, the DFT-domain input signal matrix $\mathbf{X}_\tau = \text{diag}(\underline{x}_\tau) = \text{diag}(\mathbf{F}_M \underline{x}_\tau) \in \mathbb{C}^{M \times M}$ and the zero-padding matrix $\mathbf{Q}_1^T = (\mathbf{I}_{M-R} \quad \mathbf{0}_{M-R \times R})$. Note that $\mathbf{Q}_1^T = (\mathbf{0}_{R \times M-R} \quad \mathbf{I}_R)$ ensures a linear convolution by constraining the inverse DFT of the product $\mathbf{X}_\tau \mathbf{w}_\tau$. By inserting the propagation model (4) into the signal model (2) and pre-multiplying with the transformation matrix $\mathbf{F}_M \mathbf{Q}_1$, we obtain the DFT-domain observation model

$$\mathbf{y}_\tau = \mathbf{C}_\tau \mathbf{w}_\tau + \mathbf{n}_\tau \in \mathbb{C}^M, \quad (5)$$

with $\mathbf{C}_\tau = \mathbf{F}_M \mathbf{Q}_1 \mathbf{Q}_1^T \mathbf{F}_M^{-1} \mathbf{X}_\tau$ being the overlap-save constrained input signal matrix and the DFT-domain microphone and noise blocks $\mathbf{y}_\tau = \mathbf{F}_M \mathbf{Q}_1 \underline{y}_\tau$ and $\mathbf{n}_\tau = \mathbf{F}_M \mathbf{Q}_1 \underline{n}_\tau$, respectively.

The unknown FR \mathbf{w}_τ is usually estimated by iteratively applying the update rule [24]

$$\mathbf{e}_\tau = \mathbf{y}_\tau - \hat{\mathbf{d}}_\tau = \mathbf{y}_\tau - \mathbf{C}_\tau \hat{\mathbf{w}}_{\tau-1} \quad (6)$$

$$\hat{\mathbf{w}}_\tau = \hat{\mathbf{w}}_{\tau-1} + \mathbf{Q}_3 \Lambda_\tau \mathbf{X}_\tau^H \mathbf{e}_\tau \quad (7)$$

which represents a block-based frequency-domain implementation of the least mean square (LMS) algorithm [25] and is often termed FDAF [6, 26]. Here, the preceding estimate $\hat{\mathbf{w}}_{\tau-1}$ is updated by a multiplication of the stochastic gradient $\mathbf{X}_\tau^H \mathbf{e}_\tau$, including the prior error \mathbf{e}_τ , with a diagonal step-size matrix $\Lambda_\tau \in \mathbb{R}^{M \times M}$. Note that the gradient projection matrix $\mathbf{Q}_3 = \mathbf{F}_M \mathbf{Q}_2 \mathbf{Q}_2^T \mathbf{F}_M^{-1}$ ensures that the FR estimate $\hat{\mathbf{w}}_\tau$ corresponds to a zero-padded time-domain FIR filter $\underline{\hat{w}}_\tau = \mathbf{Q}_2^T \mathbf{F}_M^{-1} \hat{\mathbf{w}}_\tau$.

3. ADAPTATION CONTROL

The convergence rate, steady-state performance and noise-robustness of the adaptive system identification algorithm described in Sec. 2 decisively depends on an accurate choice of the frequency-dependent step-sizes contained in Λ_τ . In the following, we will introduce a DNN-based method which infers the step-size matrix Λ_τ directly from the observed signals \mathbf{x}_τ and \mathbf{e}_τ as shown in Fig. 1.

3.1. Model-Based Adaptation Control

We start by discussing state-of-the-art model-based adaptation control which will serve as a motivation for the proposed method in Sec. 3.2. The vast majority of these approaches suggests a computation of the step-size matrix

$$\Lambda_\tau^{\text{MB}} = f_{\text{MB}} \left(\Psi_\tau^{\text{XX}}, \Psi_\tau^{\text{NN}}, \Psi_\tau^{\Delta \mathbf{w} \Delta \mathbf{w}} \right) \quad (8)$$

from the input signal PSD matrix $\Psi_\tau^{\text{XX}} = \mathbb{E}[\mathbf{x}_\tau \mathbf{x}_\tau^H]$, the noise signal PSD matrix $\Psi_\tau^{\text{NN}} = \mathbb{E}[\mathbf{n}_\tau \mathbf{n}_\tau^H]$ and a correlation matrix representing the FR estimation uncertainty $\Psi_\tau^{\Delta \mathbf{w} \Delta \mathbf{w}} = \mathbb{E}[\Delta \mathbf{w}_\tau \Delta \mathbf{w}_\tau^H]$ with $\Delta \mathbf{w}_\tau = \hat{\mathbf{w}}_\tau - \mathbf{w}_\tau$. Prominent examples are the classical FDAF update [6, 26]

$$\left[\Lambda_\tau^{\text{FDAF}} \right]_{mm} = \frac{\mu_{\text{FDAF}}}{\left[\Psi_\tau^{\text{XX}} \right]_{mm}} \quad (9)$$

with $\mu_{\text{FDAF}} > 0$ being a hyperparameter, and the diagonalized DFT-domain KF update [17, 19, 20]

$$\left[\Lambda_\tau^{\text{KF}} \right]_{mm} = \frac{\left[\Psi_\tau^{\Delta \mathbf{w} \Delta \mathbf{w}} \right]_{mm}}{\left[\mathbf{x}_\tau \mathbf{x}_\tau^H \right]_{mm} \left[\Psi_\tau^{\Delta \mathbf{w} \Delta \mathbf{w}} \right]_{mm} + \frac{M}{R} \left[\Psi_\tau^{\text{NN}} \right]_{mm}}, \quad (10)$$

where the latter can be considered as a noise-robust state-of-the-art approach. However, the system identification performance of these model-based approaches crucially depends on a robust estimation of the respective signal statistics (cf. Sec. 1). While the estimation of the input signal PSD matrix Ψ_τ^{XX} is straightforward due to the observability of \mathbf{x}_τ , the estimation of statistics corresponding to unobserved quantities, e.g., Ψ_τ^{NN} and $\Psi_\tau^{\Delta \mathbf{w} \Delta \mathbf{w}}$, is still a not sufficiently solved problem and has been explored extensively [19, 20].

3.2. Deep Neural Network-based Adaptation Control

We suggest to replace the model-based mapping of signal statistics to step-size matrices (cf. Eq. (8)) by a learned mapping f_{ML} of the observable input signal sequence $\mathbf{x}_1, \dots, \mathbf{x}_\tau$ and prior error signal sequence $\mathbf{e}_1, \dots, \mathbf{e}_\tau$:

$$\Lambda_\tau^{\text{DNN}} = f_{\text{ML}}(\mathbf{x}_1, \mathbf{e}_1, \dots, \mathbf{x}_\tau, \mathbf{e}_\tau; \boldsymbol{\theta}). \quad (11)$$

The parameter vector $\boldsymbol{\theta}$ of the function f_{ML} is optimized in a training phase (cf. Sec. 3.3). However, a direct estimation of $\Lambda_\tau^{\text{DNN}}$ by a DNN is complicated by the non-stationarity and non-whiteness of the respective signals. Thus, we suggest to exploit the domain knowledge from optimum model-based adaptation control (cf. Sec. 3.1), by using the following DFT bin-wise step-size

$$\left[\Lambda_\tau^{\text{DNN}} \right]_{mm} = \frac{\mu_{\text{MAX}} \left[\mathbf{M}_\tau^\mu \right]_{mm}}{\left[\hat{\Psi}_\tau^{\text{XX}} + \frac{M}{R} \hat{\Psi}_\tau^{\text{PP}} \right]_{mm}}, \quad (12)$$

with

$$\hat{\Psi}_\tau^{\text{XX}} = \lambda_X \hat{\Psi}_{\tau-1}^{\text{XX}} + (1 - \lambda_X) \mathbf{x}_\tau \mathbf{x}_\tau^H \quad (13)$$

$$\hat{\Psi}_\tau^{\text{PP}} = \lambda_P \hat{\Psi}_{\tau-1}^{\text{PP}} + (1 - \lambda_P) \hat{\mathbf{p}}_\tau \hat{\mathbf{p}}_\tau^H \quad (14)$$

$$\hat{\mathbf{p}}_\tau = \mathbf{M}_\tau^e \mathbf{e}_\tau, \quad (15)$$

where the diagonal masking matrices \mathbf{M}_τ^μ and \mathbf{M}_τ^e are inferred by the DNN and where λ_X and λ_P are time constants for recursive averaging. By embedding the signal power normalization into the structure of the learning-based step-size mapping (11), the DNN needs to model a significantly reduced dynamic range in contrast to directly estimating $\Lambda_\tau^{\text{DNN}}$. The step-size (12) is motivated by adding an error

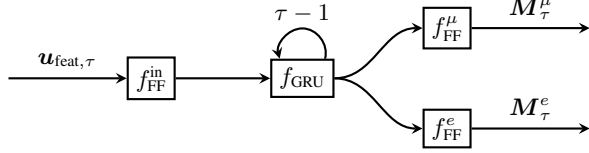


Fig. 2: Proposed DNN architecture which maps the feature vector $\mathbf{u}_{\text{feat},\tau}$ to the diagonal masking matrices \mathbf{M}_τ^μ and \mathbf{M}_τ^e .

power-dependent normalization term $\hat{\Psi}_\tau^{\text{PP}}$, similar to the noise PSD matrix Ψ_τ^{NN} in the KF update (10), to the FDAF step-size (9) and estimating the decisive hyperparameter μ_{FDAF} frequency-selectively by a DNN. To account for the different causes of large error powers, i.e., observation noise \mathbf{n}_τ or system mismatch $\Delta \mathbf{w}_\tau$, and their antipodal effect on the adaptation rate, a DNN-estimated mask \mathbf{M}_τ^e is applied to the error signal e_τ before computing $\hat{\Psi}_\tau^{\text{PP}}$ (cf. Eqs. (14) and (15)). Note that despite the structural similarity of the step-sizes (10) and (12), $\hat{\Psi}_\tau^{\text{PP}}$ is not necessarily an estimate of the noise signal PSD matrix Ψ_τ^{NN} . Its actual meaning depends on the cost function that is used to train the DNN.

We suggest the DNN architecture shown in Fig. 2 to map the observed feature vector $\mathbf{u}_{\text{feat},\tau}$ (cf. Eq. (16) below) to the diagonal masking matrices \mathbf{M}_τ^μ and \mathbf{M}_τ^e required in Eqs. (12) and (15). The architecture is motivated by the creation of a condensed feature representation after the gated recurrent unit (GRU) layer which includes all important effects influencing the adaptation control, e.g., noise activity and filter convergence state. For the input feature vector to the DNN we use the normalized logarithmic power spectrum of the input signal \mathbf{x}_τ and the prior error signal e_τ to obtain

$$[\mathbf{u}_{\text{feat},\tau}]_m = \frac{\log \max(|[\mathbf{u}_{\text{sig},\tau}]_m|^2, \epsilon) - [\boldsymbol{\nu}]_m}{[\boldsymbol{\sigma}]_m} \quad (16)$$

which is computed from the complex signal vector

$$\mathbf{u}_{\text{sig},\tau} = [(\mathbf{Q}_4 \mathbf{e}_\tau)^T \quad (\mathbf{Q}_4 \mathbf{x}_\tau)^T]^T \in \mathbb{C}^{M+2}. \quad (17)$$

The mean and element-wise standard deviation vectors of the logarithmic power spectra are denoted by $\boldsymbol{\nu}$ and $\boldsymbol{\sigma}$, respectively. Furthermore, the matrix $\mathbf{Q}_4 = \begin{pmatrix} \mathbf{I}_{\frac{M}{2}+1} & \mathbf{0}_{\frac{M}{2}+1 \times \frac{M}{2}-1} \end{pmatrix}$ selects the non-redundant part of the conjugate symmetric signals in (17) and $\epsilon > 0$ ensures a positive argument of the logarithm. The feature vector $\mathbf{u}_{\text{feat},\tau}$ is mapped by a feedforward layer with tanh activation $f_{\text{FF}}^{\text{in}}$ to a lower dimension P . Subsequently, two stacked GRU layers f_{GRU} extract temporal dependencies of the compressed feature vectors. Finally, the GRU states are mapped by two different feedforward networks f_{FF}^μ and f_{FF}^e with sigmoid activations to the diagonal entries of the masking matrices \mathbf{M}_τ^μ and \mathbf{M}_τ^e . The sigmoid activations at the output layers ensure that all elements of the masking matrices lie in the range $[0, 1]$. This contributes to the robustness of the approach by limiting the numerator of (12) to μ_{MAX} and the norm of $\hat{\mathbf{p}}_\tau$ (cf. Eq. (15)) to $\|e_\tau\|_2$. Furthermore, note that due to the conjugate symmetry of the DFT-domain representation it suffices to compute the nonredundant part of the masking matrices. An algorithmic description of the proposed DNN-FDAF update is given in Alg. 1.

Algorithm 1 Proposed DNN-FDAF update for one signal block.

- Compute prior error block e_τ by Eq. (6)
 - Compute feature vector $\mathbf{u}_{\text{feat},\tau}$ for the DNN by Eq. (16)
 - Infer masking matrices \mathbf{M}_τ^μ and \mathbf{M}_τ^e (cf. Fig. 2)
 - Compute step-size matrix $\Lambda_\tau^{\text{DNN}}$ by Eqs. (12) - (15)
 - Update FR estimate $\hat{\mathbf{w}}_\tau$ by Eq. (7)
-

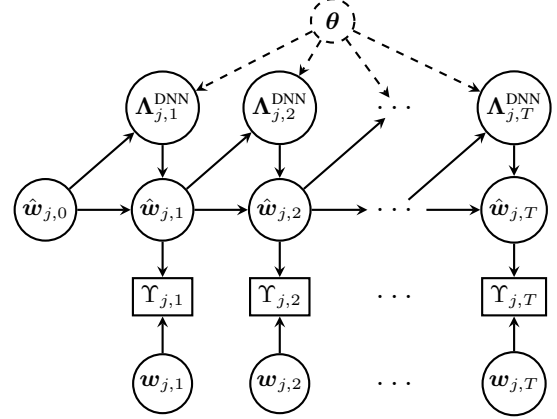


Fig. 3: Visualizing the relationship between the cost function terms $\Upsilon_{j,\tau}$ and the DNN parameter vector $\boldsymbol{\theta}$.

3.3. Cost Function Design for Neural Network Training

The system identification performance of an adaptive filter is often quantified by the NESD [1]

$$\Upsilon_\tau = \frac{\|\mathbf{w}_\tau - \hat{\mathbf{w}}_\tau\|_2^2}{\|\mathbf{w}_\tau\|_2^2}. \quad (18)$$

Due to the complex interaction of the DNN outputs, i.e., the masking matrices \mathbf{M}_τ^μ and \mathbf{M}_τ^e (cf. Fig. 2), via a sequence of filter updates (cf. Eqs. (7) and (12) - (15)) on the NESD Υ_τ , a hand-crafted design of optimum target masking matrices is problematic. Thus, we suggest an end-to-end approach by directly optimizing the DNN parameter vector $\boldsymbol{\theta}$ w.r.t. to the average logarithmic NESD

$$\mathcal{J}(\boldsymbol{\theta}) = \frac{1}{JT} \sum_{j=1}^J \sum_{\tau=1}^T 10 \log_{10}(\Upsilon_{j,\tau}), \quad (19)$$

with J and T being the number of training sequences and signal blocks, respectively, and $\Upsilon_{j,\tau}$ denoting the NESD (18) at block τ in training sequence j . The cost function (19) quantifies the direct effect of different masking matrices on the average system identification performance of the adaptive filter and renders the design of desired target signal statistics and choice of critical hyperparameters unnecessary. The end-to-end training of the DNN requires to back-propagate the average NESD (19) through the adaptive filter updates (7) to the DNN parameter vector $\boldsymbol{\theta}$. This complex relation between the cost function terms $\Upsilon_{j,\tau}$, the FR estimates $\hat{\mathbf{w}}_{j,\tau}$, the step-size matrices $\Lambda_{j,\tau}^{\text{DNN}}$ and the DNN parameters $\boldsymbol{\theta}$ is shown in Fig. 3. Finally, note that due to the independency of the NESD (18) on the signal characteristics, the cost function (19) is well-suited to quantify the system identification performance for non-stationary input signals as typically encountered in acoustic applications.

4. EXPERIMENTS

In this section, we evaluate the proposed algorithm for a large variety of challenging acoustic system identification scenarios which are motivated by an AEC application. The scenarios are characterized by abrupt changes of acoustic impulse responses (AIRs) and non-stationary and non-white input \mathbf{x}_τ and noise signals \mathbf{n}_τ . The noise-free observation component \mathbf{d}_τ of each scenario is simulated by randomly drawing an input signal \mathbf{x}_τ from a subset of the *LibriSpeech* database [27], including 143 speakers, and convolving it

with a randomly-selected true AIR $\tilde{\mathbf{w}}_\tau \in \mathbb{R}^K$ from the databases [28, 29, 30], comprising 201 different AIRs. Note that, as the length K of the true AIRs $\tilde{\mathbf{w}}_\tau$ is much larger than the modeled filter length L in all considered scenarios, we can only estimate the first L taps of $\tilde{\mathbf{w}}_\tau$, i.e., we choose $\mathbf{w}_\tau = \mathbf{Q}_5^T \tilde{\mathbf{w}}_\tau$ with $\mathbf{Q}_5^T = (\mathbf{I}_L \quad \mathbf{0}_{L \times K-L})$ in Eq. (18). Subsequently, the microphone observation \mathbf{y}_τ is computed by adding a noise signal \mathbf{n}_τ . Each noise signal consists of a superposition of a randomly selected speaker from a disjoint subset of [27], including 145 speakers, and a stationary white Gaussian signal. Both noise components are scaled to yield a random SNR, i.e., power of the noise-free component \mathbf{d}_τ w.r.t. the noise component, between -10 dB and 10 dB for the speaker, and 25 dB and 35 dB for the Gaussian component. The abrupt system change is modeled by using different AIRs, input and noise signals for creating the observations \mathbf{y}_τ before and after a specific switching time. We sampled the switching time randomly in the range $[7.2\text{s}, 8.8\text{s}]$ to preclude overfitting of the DNN to a deterministic point in time.

For all considered algorithms the sampling frequency f_s is 16 kHz and the modeled filter length and frame shift are set to $L = 2048$ and $R = 1024$, respectively. As baseline algorithms we consider the KF approach [17] and an error-aware version of the FDAF step-size (9) which is termed EA-FDAF, i.e., setting $\mathbf{M}_\tau^\mu = \mathbf{M}_\tau^e = \mathbf{I}_M$ in Eq. (12) and (15). Note that for the KF update the noise PSD matrix is computed by recursively averaging the prior error e_τ with an averaging factor of 0.5 [19, 20]. In addition, we consider two choices of the state transition parameter A , i.e., $A = 0.99$ and $A = 0.999$, as it highly affects the steady-state and reconvergence performance [18]. For the proposed DNN-FDAF algorithm we consider two additional variants which are termed DNN-FDAF ($\mathbf{M}_\tau^e = \mathbf{0}_{M \times M}$) and DNN-FDAF ($\mathbf{M}_\tau^\mu = \mathbf{I}_M$). Here, the respective quantity in brackets is fixed, i.e., it is not estimated by the DNN. The parameter settings of the considered algorithms are summarized in Tab. 1. Note that the maximum numerator step-size μ_{MAX} is chosen smaller for the DNN-FDAF ($\mathbf{M}_\tau^\mu = \mathbf{I}_M$) algorithm to compensate for the deterministic numerator of the step-size (12). The considered DNN architecture (cf. Fig. 2) has approximately 2.4 million parameters with the number of hidden GRU states at each layer being $P = 256$ and $\epsilon = 10^{-12}$. It was trained on 4.4 h of training data using the ADAM optimizer [31] with a learning rate of 10^{-3} . The normalization variables ν and σ in the feature computation (16) are estimated from the training data with the prior error statistics being approximated by the respective microphone signal statistics.

We consider the average logarithmic zero-padded NESD [1]

$$\tilde{\Upsilon}_{\text{ZP},\tau} = \frac{1}{I} \sum_{i=1}^I 10 \log_{10} \frac{\|\tilde{\mathbf{w}}_{i,\tau} - \mathbf{Q}_5 \hat{\mathbf{w}}_{i,\tau}\|_2^2}{\|\tilde{\mathbf{w}}_{i,\tau}\|_2^2} \quad (20)$$

and the average logarithmic echo return loss enhancement [1]

$$\bar{\mathcal{E}}_\tau = \frac{1}{I} \sum_{i=1}^I 10 \log_{10} \frac{\mathbb{E} [\|\mathbf{d}_{i,\tau}\|_2^2]}{\mathbb{E} [\|\mathbf{d}_{i,\tau} - \hat{\mathbf{d}}_{i,\tau}\|_2^2]} \quad (21)$$

Table 1: Parameter settings for the considered algorithms.

Algorithm	λ_X	λ_P	μ_{MAX}
EA-FDAF	0.5	0.5	0.75
DNN-FDAF ($\mathbf{M}_\tau^e = \mathbf{0}_{M \times M}$)	0.5	0.0	1.0
DNN-FDAF ($\mathbf{M}_\tau^\mu = \mathbf{I}_M$)	0.5	0.0	0.5
DNN-FDAF	0.5	0.0	1.0

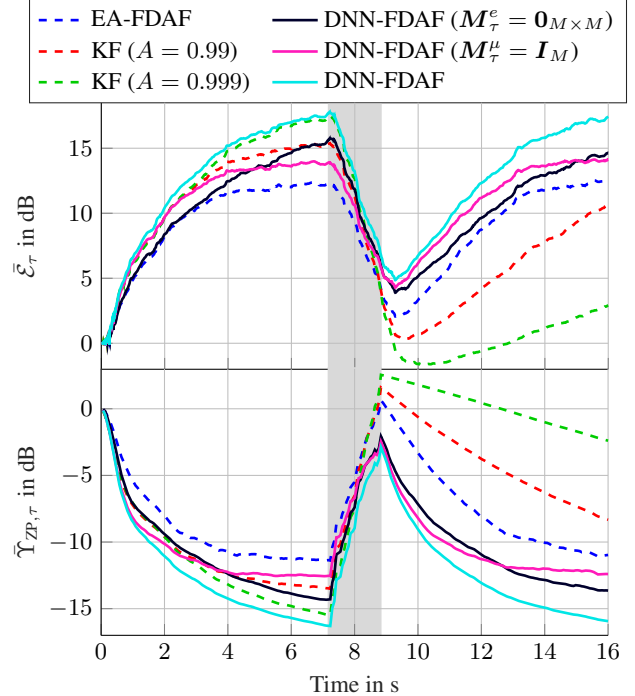


Fig. 4: Performance evaluation of the proposed DNN-FDAF algorithm, including two variants, for $I = 100$ different scenarios in comparison to various baselines. The shaded area represents the period where abrupt system changes occur at random time instants.

as performance measures with the expectation operator \mathbb{E} in (21) being approximated by recursive averaging. Note that we use a zero-padded version of the estimate $\hat{\mathbf{w}}_{i,\tau}$ in (20) to account for the undermodeling of the FIR filter model [1]. The performance measures $\tilde{\Upsilon}_{\text{ZP},\tau}$ and $\bar{\mathcal{E}}_\tau$ represent arithmetic averages of $I = 100$ different experiments (corresponding to 27 min) with varying transition times, speakers and AIRs which were disjoint from the training data.

We conclude from Fig. 4 that the proposed DNN-FDAF algorithm significantly outperforms the baselines in terms of convergence rate and reconvergence rate after abrupt AIR changes. Furthermore, while either estimating \mathbf{M}_τ^μ or \mathbf{M}_τ^e , while keeping the other one fixed, results in robust reconvergence at the cost of worse steady-state performance, their joint estimation does not need any compromise. The average runtime of the proposed DNN-FDAF algorithm for processing one signal block of duration 64 ms on an Intel Xeon CPU E3-1275 v6 @ 3.80GHz is $t_{\text{DNN}} = 1.5$ ms which confirms real-time capability on such platforms.

5. CONCLUSION

In this paper, we proposed a novel adaptation control for online system identification by using a DNN for step-size inference. By optimizing the DNN parameters end-to-end w.r.t. the average NESD of the adaptive filter, the proposed algorithm circumvents the explicit estimation of target signal statistics for model-based step-size estimation. This renders the method robust against model inaccuracies and high-level and non-stationary noise signals and avoids the need for application-dependent hyperparameter tuning. Future work may include the coupling of the proposed method with other algorithmic parts of a signal enhancement system, e.g., postfiltering.

6. REFERENCES

- [1] G. Enzner, H. Buchner, A. Favrot, and F. Kuech, "Acoustic Echo Control," in *Academic Press Library in Signal Processing*, vol. 4, pp. 807–877. Elsevier, FL, USA, 2014.
- [2] H. Zhang, K. Tan, and D. Wang, "Deep Learning for Joint Acoustic Echo and Noise Cancellation with Nonlinear Distortions," in *Interspeech*, Graz, AT, Sept. 2019, pp. 4255–4259.
- [3] N. L. Westhausen and B. T. Meyer, "Acoustic echo cancellation with the dual-signal transformation LSTM network," in *Int. Conf. Acoust., Speech, Signal Process.*, Toronto, CA, June 2021, pp. 7138–7142.
- [4] Mhd. M. Halimeh, T. Haubner, A. Briegleb, A. Schmidt, and W. Kellermann, "Combining adaptive filtering and complex-valued deep postfiltering for acoustic echo cancellation," in *Int. Conf. Acoust., Speech, Signal Process.*, Toronto, CA, June 2021, pp. 121–125.
- [5] T. Haubner, Mhd. M. Halimeh, A. Brendel, and W. Kellermann, "A Synergistic Kalman- and Deep Postfiltering Approach to Acoustic Echo Cancellation," in *European Signal Process. Conf.*, Dublin, IE, Aug. 2021.
- [6] S. Haykin, *Adaptive Filter Theory*, Prentice Hall, NJ, USA, 2002.
- [7] P. S. R. Diniz, *Adaptive Filtering: Algorithms and Practical Implementation*, Springer, Berlin, Heidelberg, 2007.
- [8] E. Hänsler and G. Schmidt, *Acoustic Echo and Noise Control: A practical Approach*, Wiley-Interscience, NJ, USA, 2004.
- [9] C. Paleologou, S. Ciochină, and J. Benesty, "Double-talk robust VSS-NLMS algorithm for under-modeling acoustic echo cancellation," in *Int. Conf. Acoust., Speech, Signal Process.*, Las Vegas, USA, Apr. 2008, pp. 245–248.
- [10] T. Gansler, M. Hansson, C.-J. Ivarsson, and G. Salomonsson, "A double-talk detector based on coherence," *IEEE Trans. Commun.*, vol. 44, no. 11, pp. 1421–1427, Nov. 1996.
- [11] J. Benesty, D. R. Morgan, and J. H. Cho, "A new class of doubletalk detectors based on cross-correlation," *IEEE Trans. Speech Audio Process.*, vol. 8, no. 2, pp. 168–172, Mar. 2000.
- [12] H. Huang and J. Lee, "A new variable step-size NLMS algorithm and its performance analysis," *IEEE Trans. Signal Process.*, vol. 60, no. 4, pp. 2055–2060, 2012.
- [13] B. H. Nitsch, "A frequency-selective stepfactor control for an adaptive filter algorithm working in the frequency domain," *Signal Process.*, vol. 80, no. 9, pp. 1733–1745, 2000.
- [14] J. Benesty, H. Rey, L. R. Vega, and S. Tressens, "A Nonparametric VSS NLMS Algorithm," *IEEE Signal Process. Lett.*, vol. 13, no. 10, pp. 581–584, 2006.
- [15] C. Huemmer, R. Maas, and W. Kellermann, "The NLMS algorithm with time-variant optimum stepsize derived from a Bayesian network perspective," *IEEE Signal Process. Lett.*, vol. 22, no. 11, pp. 1874–1878, 2015.
- [16] C. Breining, "Applying a Neural Network for Stepsize Control in Echo Cancellation," in *Proc. Int. Workshop Acoust. Echo Noise Control*, London, UK, Sept. 1997.
- [17] G. Enzner and P. Vary, "Frequency-domain adaptive Kalman filter for acoustic echo control in hands-free telephones," *Signal Process.*, vol. 86, no. 6, pp. 1140–1156, June 2006.
- [18] F. Yang, G. Enzner, and J. Yang, "Frequency-Domain Adaptive Kalman Filter With Fast Recovery of Abrupt Echo-Path Changes," *IEEE Signal Process. Lett.*, vol. 24, no. 12, pp. 1778–1782, Dec. 2017.
- [19] S. Malik and G. Enzner, "Online maximum-likelihood learning of time-varying dynamical models in block-frequency-domain," in *Int. Conf. Acoust., Speech, Signal Process.*, Dallas, USA, Mar. 2010, pp. 3822–3825.
- [20] J. Franzen and T. Fingscheidt, "Improved Measurement Noise Covariance Estimation for N-channel Feedback Cancellation Based on the Frequency-Domain Adaptive Kalman Filter," in *Int. Conf. Acoust., Speech, Signal Process.*, Brighton, UK, May 2019, pp. 965–969.
- [21] T. Jiang, R. Liang, Q. Wang, C. Zou, and C. Li, "An Improved Practical State-Space FDAF With Fast Recovery of Abrupt Echo-Path Changes," *IEEE Access*, vol. 7, pp. 61353–61362, 2019.
- [22] T. Haubner, A. Brendel, M. Elminshawi, and W. Kellermann, "Noise-Robust Adaptation Control for Supervised Acoustic System Identification Exploiting a Noise Dictionary," in *Int. Conf. Acoust., Speech, Signal Process.*, Toronto, CA, June 2021.
- [23] A. A. Nugraha, A. Liutkus, and E. Vincent, "Multichannel Audio Source Separation With Deep Neural Networks," *IEEE Audio, Speech, and Language Process.*, vol. 24, no. 9, pp. 1652–1664, Sept. 2016.
- [24] E. Ferrara, "Fast implementations of LMS adaptive filters," *IEEE Trans. Acoust.*, vol. 28, no. 4, pp. 474–475, Aug. 1980.
- [25] B. Widrow and M. E. Hoff, "Adaptive Switching Circuits," in *Proc. WESCON Conv. Rec.*, Los Angeles, USA, Aug. 1960, pp. 96–104.
- [26] J. J. Shynk, "Frequency-domain and multirate adaptive filtering," *IEEE Signal Process. Mag.*, vol. 9, no. 1, pp. 14–37, 1992.
- [27] V. Panayotov, G. Chen, D. Povey, and S. Khudanpur, "Librispeech: An ASR corpus based on public domain audio books," in *Int. Conf. Acoust., Speech, Signal Process.*, Brisbane, AUS, Apr. 2015, pp. 5206–5210.
- [28] M. Jeub, M. Schäfer, and P. Vary, "A binaural room impulse response database for the evaluation of dereverberation algorithms," in *Int. Conf. on Digit. Signal Process.*, Santorini, GR, July 2009.
- [29] J. Y. C. Wen, N. D. Gaubitch, E. A. P. Habets, T. Myatt, and P. A. Naylor, "Evaluation of speech dereverberation algorithms using the MARDY database," in *Proc. Int. Workshop Acoust. Echo Noise Control*, Paris, FR, Sept. 2006.
- [30] "Multi-channel impulse response database (MIRD)," <https://www.iks.rwth-aachen.de/en/research/tools-do> Accessed: 2020-12-04.
- [31] D. Kingma and J. Ba, "ADAM: A method for stochastic optimization," *arXiv preprint arXiv:1412.6980*, 2014.